Journal of Hepatocellular Carcinoma

Dovepress
Taylor & Francis Group

Open Access Full Text Article

ORIGINAL RESEARCH

CT Radiomics Combined with Metabolic-Biomarkers Enables Early Recurrence Prediction in Hepatocellular Carcinoma

Liying Ren[1,2,*], Dongbo Chen[2,*], Tingfeng Xu[3,*], Rongyu Wei[1], Bigeng Zhao[1], Yuanping Zhou[4], Yong He[5], Minjun Liao[2], Hongsong Chen[2], Weijia Liao[1]

[1]Laboratory of Hepatobiliary and Pancreatic Surgery, the First Affiliated Hospital of Guilin Medical University, Guilin, Guangxi, People's Republic of China; [2]Peking University Hepatology Institute, Peking University People's Hospital, Beijing Key Laboratory of Hepatitis C and Immunotherapy for Liver Disease, Beijing, People's Republic of China; [3]Affiliation Department of Hepatobiliary Surgery, the First Affiliated Hospital of Guangxi Medical University, Nanning, Guangxi, People's Republic of China; [4]Guangdong Provincial Key Laboratory of Gastroenterology, Department of Gastroenterology and Hepatology Unit, Nanfang Hospital, Southern Medical University, Guangzhou, Guangdong, People's Republic of China; [5]Department of Radiology, the Second Affiliated Hospital of Guilin Medical University, Guilin, Guangxi, People's Republic of China

*These authors contributed equally to this work

Correspondence: Weijia Liao, Laboratory of Hepatobiliary and Pancreatic Surgery, the First Affiliated Hospital of Guilin Medical University, No. 15, Lequn Road, Xiufeng District, Guilin, Guangxi, 541001, People's Republic of China, Email liaoweijia288@163.com; Hongsong Chen, Peking University Hepatology Institute, Peking University People's Hospital, No. 11 Xizhimen South Street, Beijing, 100044, People's Republic of China, Email chenhongsong2999@163.com

Journal of Hepatocellular Carcinoma downloaded from https://www.dovepress.com/
For personal use only.

Background: The prognosis of early recurrence of hepatocellular carcinoma (HCC) remains poor. This study aimed to develop and validate a radiomics model and determine potential biomarkers involved in biological pathways for early recurrence of HCC.

Methods: A total of 271 HCC patients from the First Affiliated Hospital of Guilin Medical University were enrolled as the training cohort. Recurrence related radiomics features were determined by analyzing contrast-enhanced CT images, which were used for the construction of Rad-score. For external validation, we utilized both imaging and transcriptome data from 34 HCC patients in TCGA database. The identified radiomics-related genes were further validated using two independent datasets (OEP000321 and GSE14520) and immunohistochemical analysis of EEF1E1 in 38 HCC tissue samples from training cohort.

Results: Rad-scores based on six radiomics features showed predictive value for early HCC recurrence in both cohorts (*A465, A466, A839, V105, V250, V291*). Relevant radiomics features are associated with metabolism, proliferation, and immune pathways. The most relevant recurrence-related radiomics gene module was determined via weighted correlation network analysis (WGCNA), which contained LRP12, GPD1L, GARS, EEF1E1, and DGKG. The model based on these genes could efficiently predict early HCC recurrence and was verified in the OEP000321 and GSE14520 datasets. Moreover, EEF1E1 was significantly associated with the Rad-score, illustrated prognostic value at the transcription level, and validated by immunohistochemical staining at the protein level.

Conclusion: Rad-score and radiomics gene signatures from enhanced CT effectively predicted early recurrence in HCC, while EEF1E1 might serve as an efficient biomarker for early recurrence prediction for hepatocellular carcinoma.

Keywords: contrast-enhanced CT, hepatocellular carcinoma, radiomics, early recurrence, EEF1E1

Introduction

Hepatocellular carcinoma (HCC) ranks sixth in incidence and third in mortality around the world,[1] and the early recurrence rate of HCC remains high.[2] Although serum alpha-fetoprotein (AFP) is an effective biomarker for HCC diagnosis and recurrence monitoring,[3–5] there are still some limitations. At present, some prognostic prediction models have been developed based on HCC image data,[6,7] and their accuracy are better than that of the traditional model.[8] Even though there are important reference values for the molecular genotype of patients with HCC for individualized treatment, the biological significance of the radiomics features has not been elucidated. Annotation of biological

Received: 15 June 2025
Accepted: 16 September 2025
Published: 29 September 2025

© 2025 Ren et al. This work is published and licensed by Dove Medical Press Limited. The full terms of this license are available at https://www.dovepress.com/terms.php and incorporate the Creative Commons Attribution – Non Commercial (unported, v4.0) License (http://creativecommons.org/licenses/by-nc/4.0/). By accessing the work you hereby accept the Terms. Non-commercial uses of the work are permitted without any further permission from Dove Medical Press Limited, provided the work is properly attributed. For permission for commercial use of this work, please see paragraphs 4.2 and 5 of our Terms (https://www.dovepress.com/terms.php).

Graphical Abstract

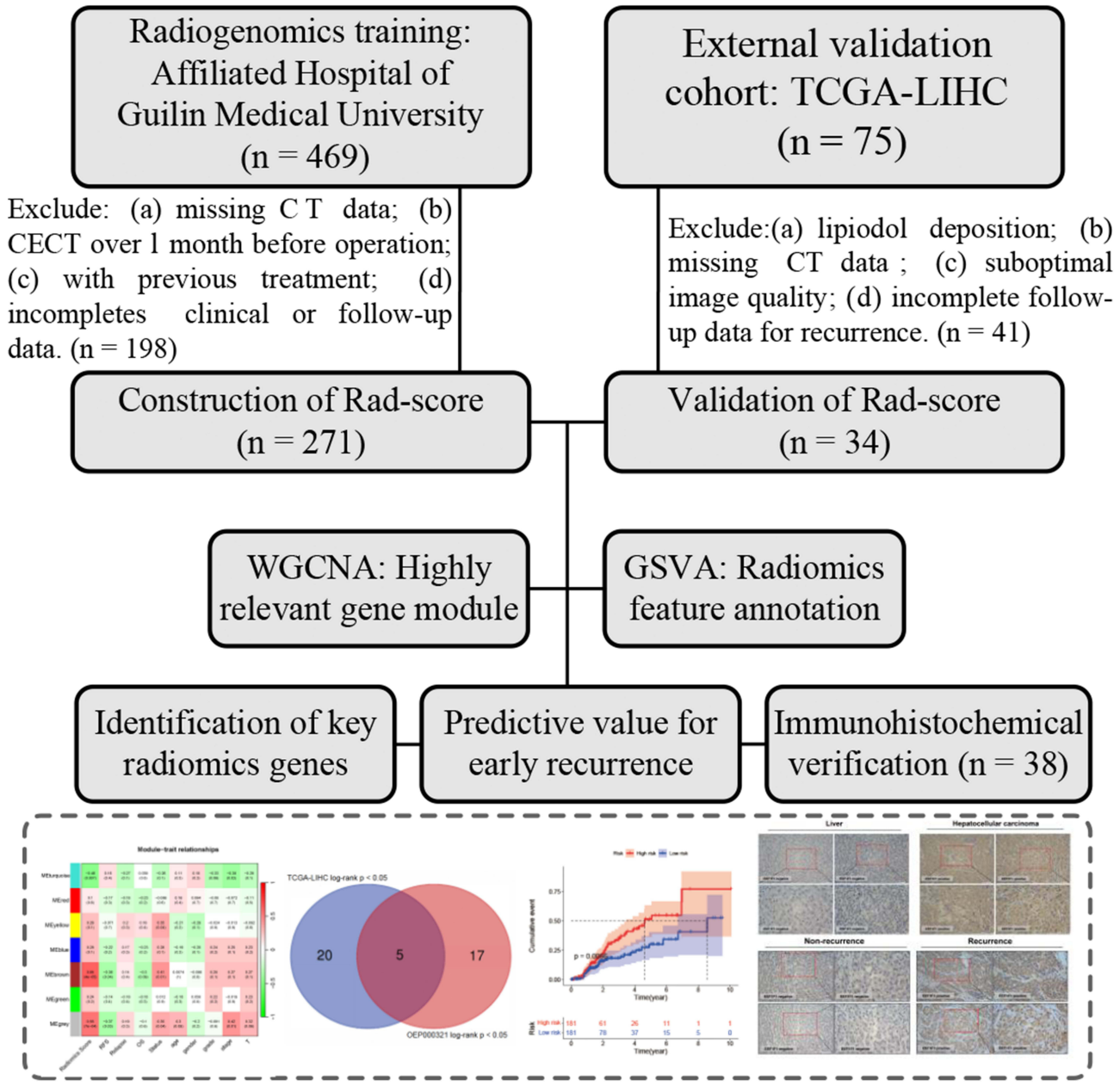

pathways related to radiomics features and further understanding of the underlying key genes might effectively guide the clinical implementation of precision therapy for patients with HCC.

After a decade of development, radiomics has been widely used for disease diagnosis,[9] efficacy evaluation, and prognosis prediction.[10] Although radiogenomics methods are necessary, they are rarely used to reveal the underlying mechanism for early recurrence of HCC. Microvascular invasion (MVI) is an independent risk factor for recurrence and metastasis of HCC.[11] Previous studies have used ultrasound (US), enhanced CT, or other modalities to predict MVI, and the results were better than those of traditional biomarkers.[12–16] Radiomics has a good predictive effect on overall survival (OS) and recurrence, as well.[7,17] Although some studies have explored the changes in certain pathways or

mechanisms through radiomics,[18,19] few studies have annotated the radiomic features of HCC through transcriptome data. To the best of our knowledge, no studies have examined the relationship between gene expression and the Rad-score.

Despite encouraging prognostic performance, most existing HCC radiomics models function as black-box predictors and rarely connect quantitative image signatures to tractable biology, which hampers clinical translation and treatment selection. To address this unmet need, we integrate contrast-enhanced CT radiomics with transcriptomic profiling to annotate recurrence-related features by pathways and distill a compact, biologically interpretable gene set, further supported by protein-level IHC validation. This design aims to bridge prediction and mechanism, thereby improving the rationale for model use in decision-making.

In this study, we aimed to develop a radiomics model based on contrast-enhanced CT imaging for early recurrence prediction in HCC. Furthermore, we integrated transcriptomic analysis to explore radiomics-associated biological pathways, with the goal of improving the clinical applicability and translational value of radiomics in HCC management.

Materials and Methods

Study Population and Follow-up Surveillance

In our study, we retrospectively enrolled 469 patients with HCC from the First Affiliated Hospital of Guilin Medical University from October 2013 to September 2019, and 271 patients met the requirements and were set as the radiomics training dataset. Among the 271 patients, 38 HCC tissues with corresponding clinical data were randomly collected for immunohistochemistry (IHC) staining to validate the radiomics genes. We also integrated the CT imaging data of HCC from The Cancer Imaging Medicine Archive (TCIA) with RNA sequencing and clinical data from The Cancer Genome Atlas (TCGA) (https://www.cancer.gov/tcga). We matched the TCIA imaging data with TCGA genomic and clinical data, containing 34 HCC patients who met the requirements and were used to create a unified dataset referred to as the TCGA validation cohort. Furthermore, contrast-enhanced CT image data in both datasets, including the arterial and portal venous phases, and the transcription data in TCGA were obtained from the RNA sequence. In the external validation dataset, postoperative surveillance was conducted according to our previous study;[20] recurrence within two years postoperatively was defined as early recurrence. This study was reviewed and approved by the research ethics committee of the First Affiliated Hospital of Guilin Medical University and complied with The Declaration of Helsinki Principles. Written informed consent was obtained from all patients for their data to be used in the study.

Diagnostic Criteria and Exclusion Criteria

For patients in the external validation dataset enrolled from the First Affiliated Hospital of Guilin Medical University, the diagnosis criteria and radical hepatectomy criteria of the patients were described in detail in our previous study.[20] In the TCGA cohort, patients with (a) lipiodol deposition, (b) missing CT images, (c) suboptimal image quality or (d) missing follow up of recurrence were excluded. The main exclusion criteria in the external validation cohort were as follows: (a) unavailable contrast-enhanced CT image; (b) contrast-enhanced CT scan over one month before surgery; (c) previous treatment, including hepatectomy, ablation, or TACE; and (d) incomplete clinical or follow-up data.

CT Image Acquisition, the Regions of Interest (ROIs) Segmentation and Radiomics Features Extraction

Multidetector CT scanners, including GE Light Speed 64-, 128-, and 256-slice spirals, were used to conduct contrast-enhanced CT scans. Arterial phase imaging utilized contrast medium tracking, with the trigger automatically positioned at the lower border of the thoracic aorta and set at a threshold of 180 HU. A 5-second delay was implemented before image acquisition. Subsequently, the venous phase commenced with a 30-second delay after the conclusion of arterial phase scanning. The CT scanning parameters were 120 kVp, automatic tube current modulation (mA), Noise Index of 8, and a 1.25 mm interval. Standardization of images in both the arterial and venous phases was achieved through z-score normalization to attain a standard normal distribution of image intensities. The images were then resampled to voxels of $1 \times 1 \times 1$ mm^3 using Python (v3.7, https://www.python.org) and the open-source Simple-ITK package. The ROIs were

defined as the tumor areas in both the arterial and venous phases, which were delineated using 3D Slicer (v4.11, https://www.slicer.org) by two experienced radiologists with 8 and 10 years of clinical experience, respectively. In cases of disagreement, a third senior radiologist (10 years of experience) was consulted, and the final ROIs were determined by majority vote. All readers were blinded to clinical and pathological information to minimize potential bias. Radiomics feature extraction was then performed using the PyRadiomics package (v2.2.0), and a total of 1898 features were obtained, including first-order statistics, texture features, and wavelet decompositions.

The Construction and Validation of Rad-Scores and Radiomics Phenotypes

A total of 1898 contrast-enhanced CT-based radiomics features were extracted from both the arterial and portal venous phases of 271 patients in the training cohort. We then performed Minimum Redundancy Maximum Relevance (mRMR) as a pre-filtering step, and 195 of them were considered as stable features, which were, respectively, coded as *A465, A466, A839, V105, V250*, and *V291*. The coefficients of radiomics features Rad-score of each patient cohort was determined according to the coefficients of the radiomics features.

Identification of Radiomics Gene Co-Expression Module and Key Radiomics Genes

For patients in the TCGA dataset, matched transcriptome data were obtained. To reveal biological pathways, weighted correlation network analysis (WGCNA) was performed. By clustering the co-expression genes into modules, we analyzed the correlation between gene modules and different radiomic phenotypes. Highly relevant and significantly related gene modules considered as radiomics gene modules were selected for further analysis. To determine the most relevant radiomics genes, we performed a Log rank test for early recurrence among the two independent cohorts, and five intersection genes were identified as key radiomics genes. The correlation between radiomics features and radiomics genes was analyzed by Pearson; $p < 0.05$ was considered statistically significant.

Biological Pathways Underlying Different Radiomics Phenotypes

Potential biological pathways of radiomics phenotypes were evaluated using gene set variation analysis (GSVA),[21] and the enrichment score for a specific gene set was calculated for each sample. The limma package was used to perform differential analyses. Immune cell infiltration was assessed using CIBERSORT (https://cibersort.stanford.edu/). The coefficients of correlation among radiomics features, radiomics genes, and immune cell infiltration were assessed by Pearson, with $p < 0.05$ indicating a significant correlation.

Immunohistochemistry Validation of the Key Radiomics Gene

A total of 38 HCC tissues randomly selected from our independent cohort were subjected to IHC. The main steps were as follows: rabbit anti-human EEF1E1 (Proteintech Cat No: 10805-1-AP, 1:200 dilution) was incubated at 4°C overnight, followed by incubation with horseradish peroxidase (HRP)-conjugated secondary antibody (ZSGB-BIO, ZB-2301) for one h at 37°C, and staining with 3,3-diaminobenzidine tetrahydrochloride (DAB).

The stained tissue was scored by two pathologists on the following criteria: (I) staining intensity: 0 (negative, no staining), 1 (weak, faint yellow staining), 2 (moderate, yellow staining), and 3 (strong, brown staining); (II) percentage of positive cells: 0 (0%), 1 (1–10%), 2 (11–50%), 3 (51–80%), and 4 (80–100%). The IHC score of EEF1E1 expressed in HCC was calculated as follows: staining intensity score × the percentage score of positive cells, and graded as follows: IHC score ≤ 4 points was considered EEF1E1 negative while > 4 points were considered positive.

Statistical Analysis

Continuous variables that follow a normal distribution are shown as mean ± standard deviation (SD) and were compared using Student's *t*-test. Otherwise, the Mann–Whitney *U*-test was performed. Categorical variables were compared using the chi-square test. RFS analyses were conducted using the Kaplan-Meier method and Log rank test among the different groups. Time-dependent receiver operating characteristic (ROC) curves were plotted using the timeROC package. Harrell's C-index was calculated using 1000 bootstraps. Gene co-expression modules were determined using the WGCNA package.

Results

Patient Characteristics and Workflow

Initially, 469 patients from the First Affiliated Hospital of Guilin Medical University and 75 patients from the TCGA dataset were enrolled in this study. After screening according to the admission and discharge criteria, 271 patients from the First Affiliated Hospital of Guilin Medical University were included in the training cohort, while 34 patients from the TCGA dataset were set as the validation cohort and were used to explore relevant biomarkers and biological pathways.

The baseline information is shown in Table 1. Most HCC patients in the training cohort had liver cirrhosis (90.0%) and tumor size > 5 cm (73.1%). In the validation cohort, the proportion of patients aged ≥ 65 years was 50.0% (17/34), while males accounted for 55.9% (19/34).

Construction and Validation of Radiomics Phenotypes

In the training cohort comprising 271 patients, 1898 radiomics features were extracted from contrast-enhanced CT scans across arterial and portal venous phases. Following minimum redundancy maximum relevance (mRMR) feature selection, 195 features demonstrated stability, with six features (*A465, A466, A839, V105, V250, V291*) ultimately retained to construct the radiomics signature (Rad-score). The Rad-score, calculated using weighted coefficients of these features (Table S3), achieved a concordance index (C-index) of 0.796 (95% CI: 0.702–0.884) in the training cohort, outperforming individual feature predictive values (Figure 1A).

Stratification by median Rad-score identified distinct recurrence risk profiles. In the training cohort, high-risk patients (median recurrence-free survival [RFS]: 15.5 months) exhibited significantly worse outcomes compared to low-risk counterparts (median RFS: 24.9 months; Figure 1B). This prognostic discrimination was validated externally, with high-risk patients in the validation cohort demonstrating a mean RFS of 8.7 months versus 33.9 months in low-risk patients (Figure 1C). Temporal predictive accuracy was robust, with Rad-score AUCs of 0.915 (95% CI: 0.796–1.000) and 0.794 (95% CI: 0.731–0.858) for early recurrence prediction in training and validation cohorts, respectively (Figures 1D and E). As shown in Figure 1F, patients were stratified into high- and low-risk groups according to the Rad-score, with a higher proportion of recurrence observed in the high-risk group.

Clinically, Rad-score stratification correlated strongly with established prognostic indicators. Higher Rad-scores were associated with early recurrence status (Figure 1G), elevated serum alpha-fetoprotein (AFP) levels (Figure 1H), and multifocal tumors (Figure 1I). These findings collectively underscore the Rad-score's capacity to integrate tumor biological behavior with quantitative imaging phenotypes, providing a clinically actionable metric for recurrence risk stratification.

Table 1 The Clinicopathological Characteristics of HCC Patients Based on Training and Validation Cohort

Clinical Characteristics	Training (n = 271)	Validation (n = 34)	*p*-value
Age (<65/≥65)	240/31	17/17	< 0.05
Gender (male/female)	232/39	19/15	< 0.05
Liver cirrhosis (present/absent)	244/27	NA	NA
Tumor size (<5cm/≥5cm)	73/198	NA	NA
Node metastasis (N0/N1/unknow)	259/3/9	26/1/7	< 0.05
Distant metastasis (M0/unknow)	271/0	34/0	NA
BCLC stage (0+A/B+C)	147/124	NA	NA
Histologic grade (G1/G2/G3/G4)	48/147/76/0	5/15/14/0	0.543
TNM stage (I/II/III/IV)	47/88/133/3	18/4/11/1	< 0.05
Early recurrence (present/absent)	155/116	25/9	0.068

Abbreviations: NA, not applicable; BCLC, Barcelona Clinic Liver Cancer; TNM, tumor-node-metastasis.

https://doi.org/10.2147/JHC.S547186

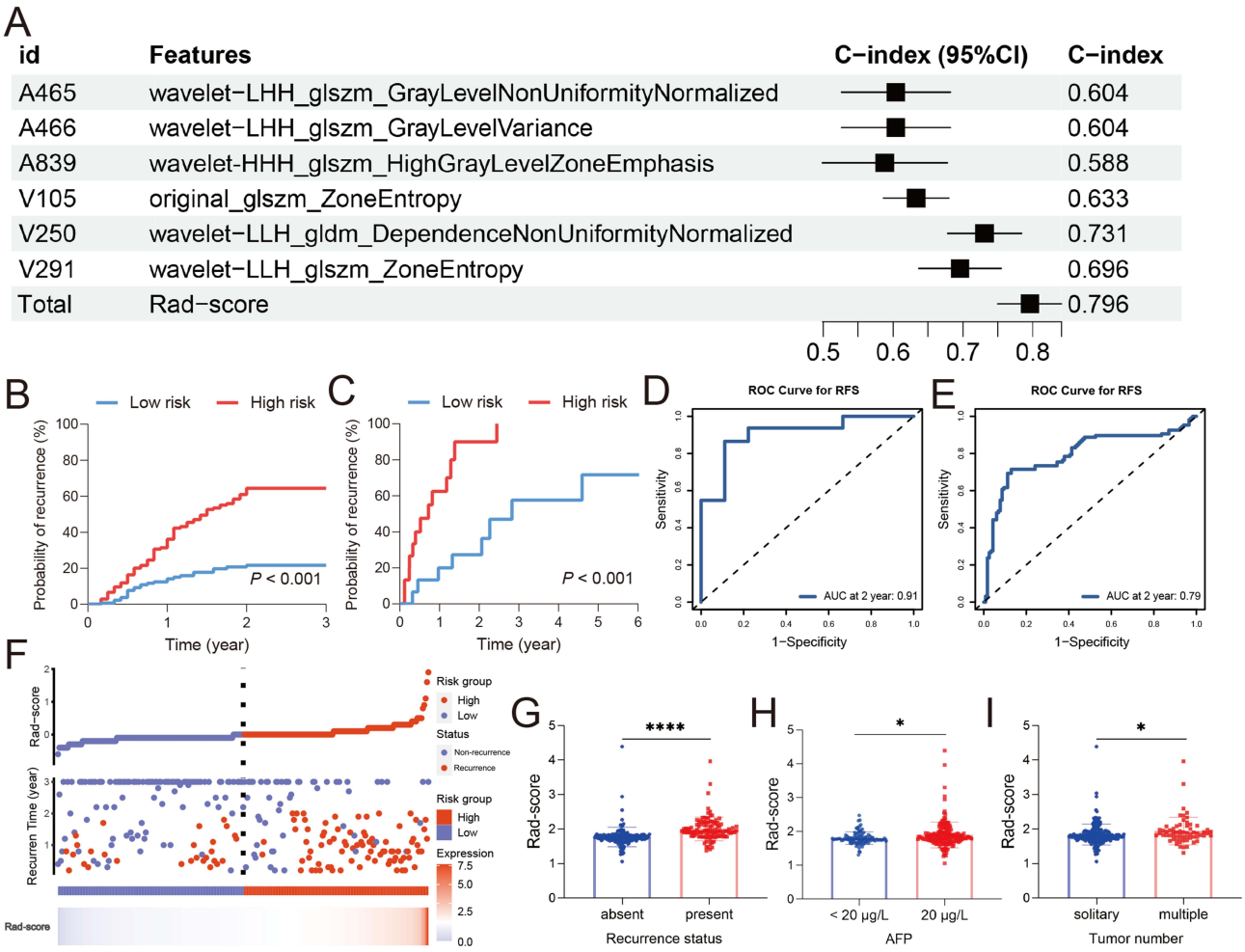

Figure 1 Construction and validation of the Rad-score for the early recurrence of HCC. (**A**) C-index of the early recurrence-related radiomics features. (**B**) Survival curve for RFS in training cohort and validation cohort (**C**). ROC curves for early recurrence in training (**D**) cohort and validation cohort (**E**). (**F**) recurrence distribution stratified by Rad-score. Rad-score was correlated recurrence status (**G**), AFP levels (**H**) and tumor number (**I**). (*$p < 0.05$, ****$p < 0.0001$).

Construction of Radiomics Gene Co-Expression Module

To elucidate the genes underlying the two risk groups, we utilized weighted gene co-expression network analysis (WGCNA) to construct a radiogenomic gene module. Differentially expressed genes (DEGs) between the groups (Figure S1) were identified and used for co-expression network construction. Hierarchical clustering revealed coherent TCGA sample groupings, and the aligned trait heatmap maps phenotype, radiomics score, survival (RFS/OS), and clinicopathologic features (Figure S2). The TOM dendrogram and network heatmap showed block-diagonal patterns, indicating strong intra-module connectivity and well-defined co-expression modules (Figure S3). The optimal soft threshold power ($\beta = 5$) was selected based on scale independence (Figure 2A), resulting in the identification of 7 distinct gene modules in the TCGA radiogenomic cohort (Figure 2B and C). These modules contained genes ranging from 40 to 134, with the brown module (99 genes) (Table S1) exhibiting the strongest positive correlation to the high-risk group ($r = 0.64$, $p < 0.001$; Figure 2C). Further analysis based on eigengene expression confirmed that the brown module was also significantly associated with the Rad-score (Figure 2G).

Within the brown module, strong concordance was observed between Module Membership (MM) and Gene Significance (GS) ($r = 0.40$, $p < 0.001$; Figure 2E), highlighting the module's relevance to the risk stratification. To better understand its biological function, GO and KEGG pathway enrichment analyses were performed. The GO analysis revealed significant enrichment in pathways related to acylglycerol, neutral lipid metabolic processes, and triglyceride

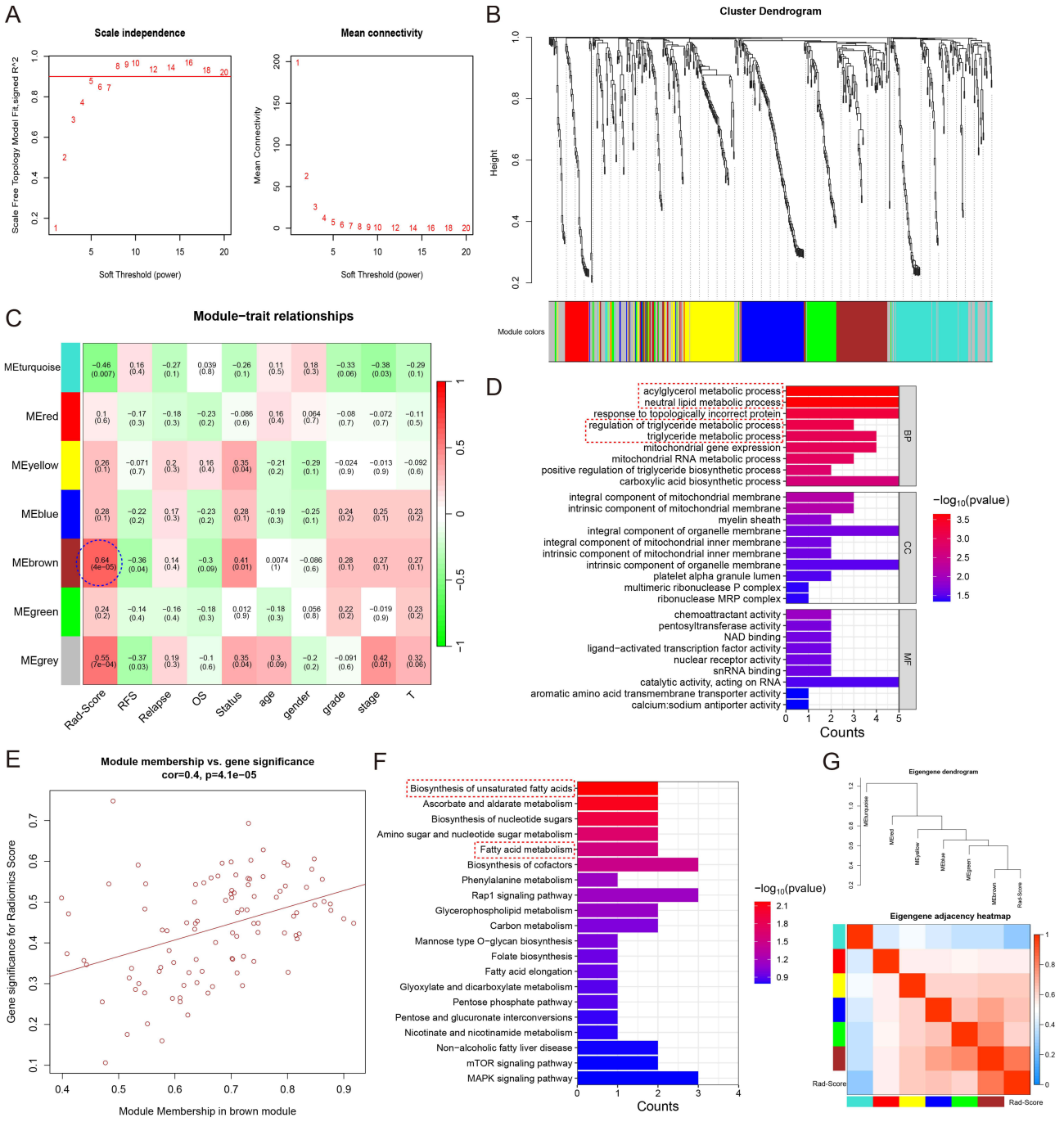

Figure 2 Weighted Correlation Network analysis (WGCNA) of the radiomics gene modules. (**A**) Scale Independence and mean connectivity showed that the optimal soft threshold is 5. (**B**) 7 gene modules were generated according to the cluster dendrogram. (**C**) A module trait association was illustrated by each row corresponding to the eigengene associated with a module in the module trait relationships. (**D**) GO enriched analysis of the patients in different radiomics phenotypes. (**E**) The MM vs GS significance for brown module was plotted to indicate the relationship between the Rad-scores and brown module. (**F**) KEGG enriched analysis of the patients in different radiomics phenotypes. (**G**) Eigengene dendrogram and heatmap were plotted to identify the radiomics gene module.

metabolic processes ($p < 0.001$), while KEGG analysis identified pathways such as the biosynthesis of unsaturated fatty acids (hsa01040, $p = 0.007$) and fatty acid metabolism (hsa01212, $p = 0.028$) (Figure 2D). These findings suggest that lipid metabolism may play a critical role in discriminating between different risk groups.

https://doi.org/10.2147/JHC.S547186

Identification of Key Radiomics Genes and Feature Annotation

Based on the intersection of Log rank test results across two independent datasets among genes in brown gene module, we identified five key radiomics genes: LRP12, GPD1L, GARS, EEF1E1, and DGKG, which were consistently significant in predicting early recurrence (Figure 3A). Since these genes were identified through their association with different risk groups, we first analyzed their correlations with radiomics features. EEF1E1 and DGKG exhibited significant positive correlations with feature *A839*, while GPD1L, GARS, EEF1E1, and DGKG were significantly positively correlated with *V250* and the Rad-score (Figure 3B). To assess their predictive value for early recurrence, we developed a linear model and stratified patients into high- and low-risk groups. Survival analysis demonstrated significant differences between these groups in both the TCGA-LIHC ($p = 0.036$) and OEP000321 ($p = 0.011$) cohorts, with the high-risk group showing a higher likelihood of early recurrence (Figure 3C and D).

To investigate underlying biological mechanisms, we examined transcriptomic differences between the risk groups. Genes from the brown module, which play a central role, were expressed at higher levels in the high-risk group, characterized by poorer prognosis and higher recurrence rates (Figure S4A). By using GSVA to quantify pathway activity, we found significant differences in pathway enrichment between the groups, with key pathways annotated in the

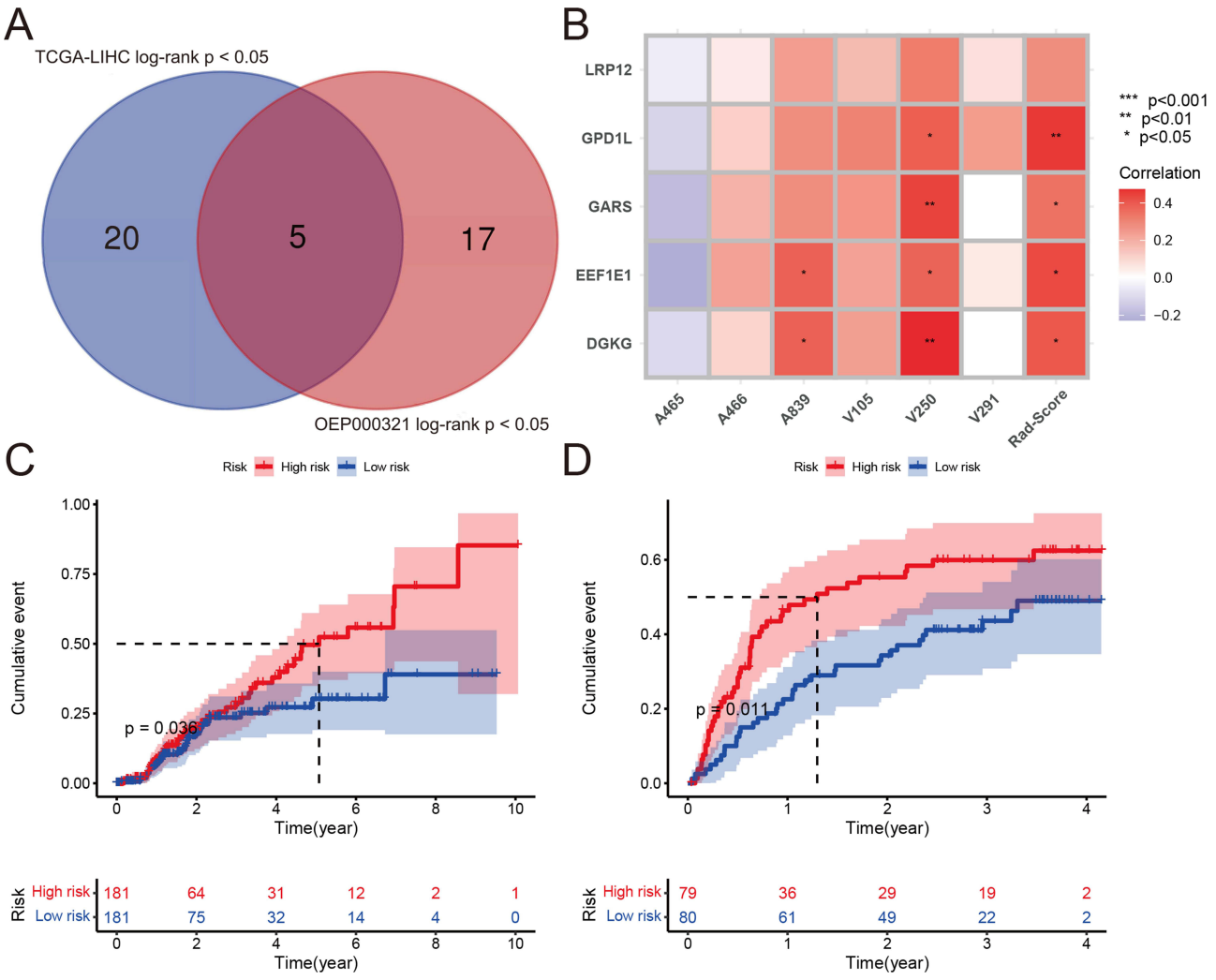

Figure 3 Radiomics genes and their predictive value for early recurrence. (**A**) Venn diagrams to determine key radiomics genes. (**B**) Correlation between key radiomics genes and features. (**C**) Risk accumulation curve of the radiomics gene signature for early recurrence in TCGA-LIHC. (**D**) Risk accumulation curve of the radiomics gene signature for early recurrence in OEP000321. (*$p < 0.05$, **$p < 0.01$, ***$p < 0.001$).

Table 2 Pathway Annotation of the Early-Recurrence Related Radiomics Features

Features	Biologic Functions	Pathways Annotations
A465	Metabolism	Fatty acid elongation; insulin glucose pathway; HIF1α pathway; AKT1 signaling via mTOR
A466	Proliferation	MYC oncogenic signature; PTEN regulation; regulation of IGFR signaling pathway
A839	Proliferation	Cell cycle arrest; cell cycle checkpoint; negative regulation of mitotic cell cycle; PI3K AKT mTOR signaling
V105	Immune	Negative regulation of adaptive immune response; regulation of T cell mediated cytotoxicity; regulation of T helper1 cell differentiation
V250	Immune	VEGFR signaling pathway; PD-1 signaling; IL-4 production; IL-6 secretion; NK cell activation; cellular response to VEGF stimulus
V291	Immune	Regulation of T cell differentiation; T cell apoptotic process; positive regulation of T cell cytokine production; CD8 positive alpha beta T cell activation

Abbreviations: HIF1α, hypoxia inducible factor 1 subunit alpha; AKT1, AKT serine/threonine kinase 1; MYC, MYC Proto-Oncogene; PTEN, phosphatase and tensin homolog; IGFR, insulin like growth factor receptor; mTOR, mechanistic target of rapamycin kinase; PD-1, programmed cell death 1; IL-6, interleukin 6; NK, natural killer, VEGF, vascular endothelial growth factor; CD8, cluster of differentiation 8.

feature heatmap (Figure S4B). These analyses offer insights into the molecular underpinnings of radiomics features and their relationship to recurrence in HCC.

Immune microenvironment analysis revealed notable associations between radiomics features and immune cell infiltration. Specifically, *A465* and *A466* were correlated with M0 macrophage infiltration, (Figure S5). All five radiomics genes were positively correlated with M0 macrophages, and notably, EEF1E1 was negatively correlated with M1 macrophages but positively correlated with M2 macrophages (Figure S6), suggesting its role in facilitating an immunosuppressive microenvironment. Additionally, these genes were associated with NK cell activity, either resting or activated, further emphasizing their relevance to immune dynamics in HCC.

The biological relevance of individual radiomics features is summarized in Table 2, detailed information was provided in the Table S2. For example, A465 appears to be involved in fatty acid and carbohydrate metabolism, potentially regulated by HIF1α, which influences energy metabolism and angiogenesis. *A465* was linked to pathways such as MYC, PTEN, and IGFR, which are key regulators of cellular proliferation. A839 was primarily associated with cell cycle regulation, indicating its role in promoting proliferation. Immune-related features: *V105, V250*, and *V291*, which play critical roles in T cell-mediated responses and immunomodulation. Notably, *V105* and *V291* were linked to T cell activation and differentiation, while *V250* was correlated with VEGF receptor signaling, PD-1 signaling, and interleukin secretion, pathways directly connected to current therapeutic strategies in HCC. These findings underscore the multifaceted roles of radiomics features in metabolism, proliferation, and immune regulation.

EEF1E1 Showed Prognostic Value and Correlation with Rad-Score

Given that DGKG has been reported to be involved in angiogenesis in HCC,[22] EEF1E1 was selected for subsequent validation. Initially, we observed differential expression of EEF1E1 at the transcriptional level and found that in three independent datasets, the expression of EEF1E1 was significantly higher in HCC tissues than in para-cancer tissues, as shown in Figure 4A–C. Next, recurrence risk accumulation curves were plotted in two of the cohorts above, patients with high EEF1E1 expression are more prone to early recurrence as shown in Figure 4D and E (log-rank $p = 0.006$ in TCGA-LIHC cohort; $p = 0.023$ in OEP000321 cohort). And there was a significant positive correlation between the mRNA level of EEF1E1 and the Rad-score (Figure 4F) (Pearson, $r = 0.455$, $p = 0.0068$). Moreover, Immunohistochemical staining suggested higher EEF1E1 protein expression in HCC tissues than in para-cancer tissues, as shown in Figure 4G.

Patients with Higher EEF1E1 Expression Were Prone to Recurrence

To further explore the relationship between the radiomic gene EEF1E1 and HCC recurrence, immunohistochemical staining was performed on 38 HCC tissues. Among all HCC samples, recurrence occurred in 18 patients (47.37%), and EEF1E1 positive rate was 39.47%. As shown in Figure 5B, the results of the chi-square test showed a significant difference in the

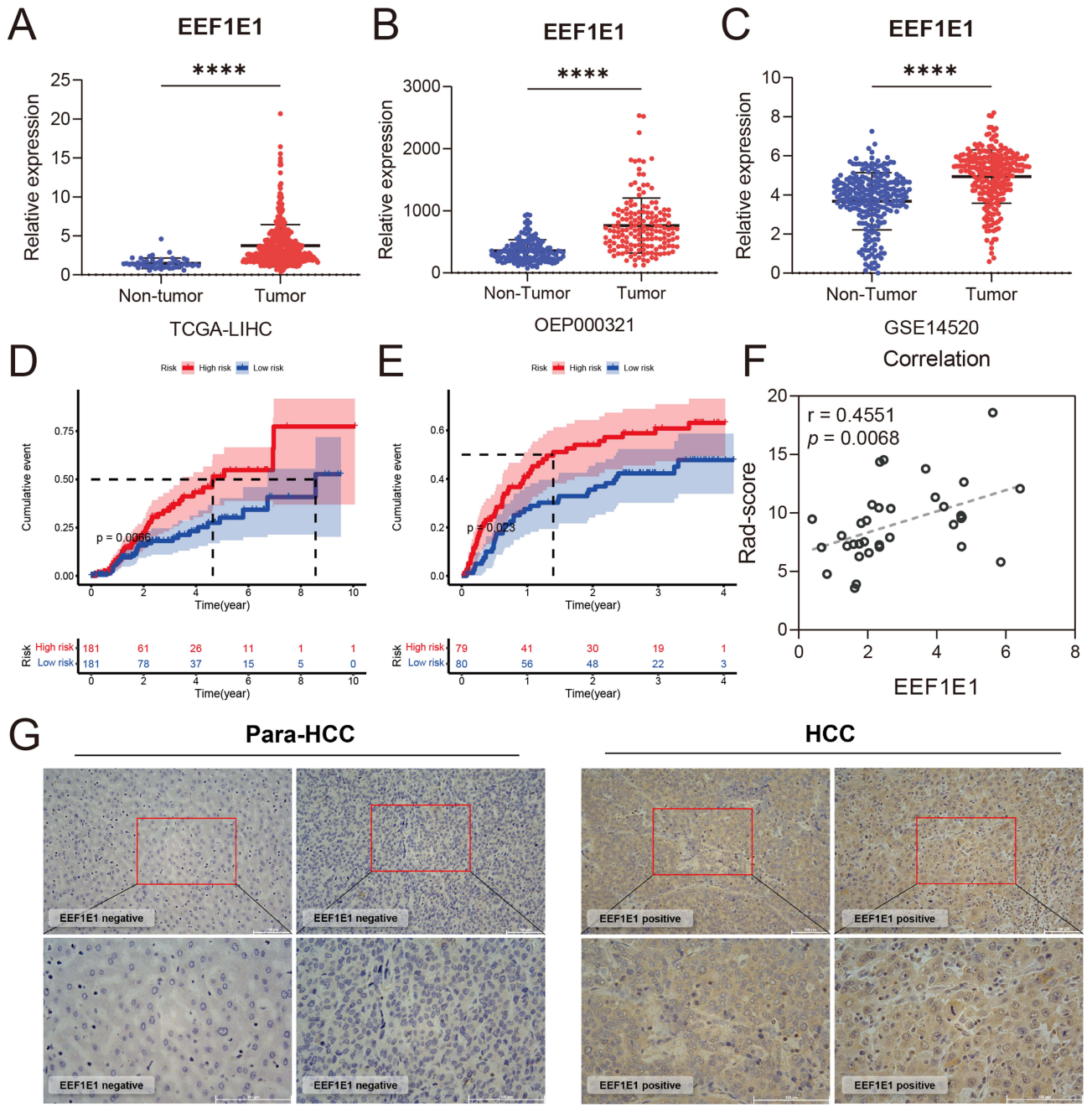

Figure 4 Differential expression and prognostic value of EEF1E1. (**A**) Differential expression of EEF1E1 in TCGA-LIHC cohort, (**B**) OEP000321 cohort and (**C**) GSE14520 cohort. (**D**) Risk accumulation curve of EEF1E1 mRNA expression for early recurrence in TCGA-LIHC and (**E**) OEP000321 cohort. (**F**) Correlation between EEF1E1 mRNA expression with Rad-scores. (**G**) IHC stains image of EEF1E1 protein levels in HCC and para cancer tissues. (****$p < 0.0001$).

protein levels of EEF1E1 in patients with and without recurrence ($p = 0.010$). Figure 5A shows the IHC staining of EEF1E1 in samples with different recurrence risks. The boxplot suggests that there were different IHC scores in the non-recurrence and recurrence risk groups (Figure 5C). The risk accumulation curve showed a higher risk in the EEF1E1 positive group, as well (Figure 5D). Moreover, there was a significant positive correlation between the EEF1E1 IHC scores and Rad-scores ($r = 0.42$, $p = 0.0084$) (Figure 5E). These results suggest that patients with EEF1E1 positive expression are prone to recurrence.

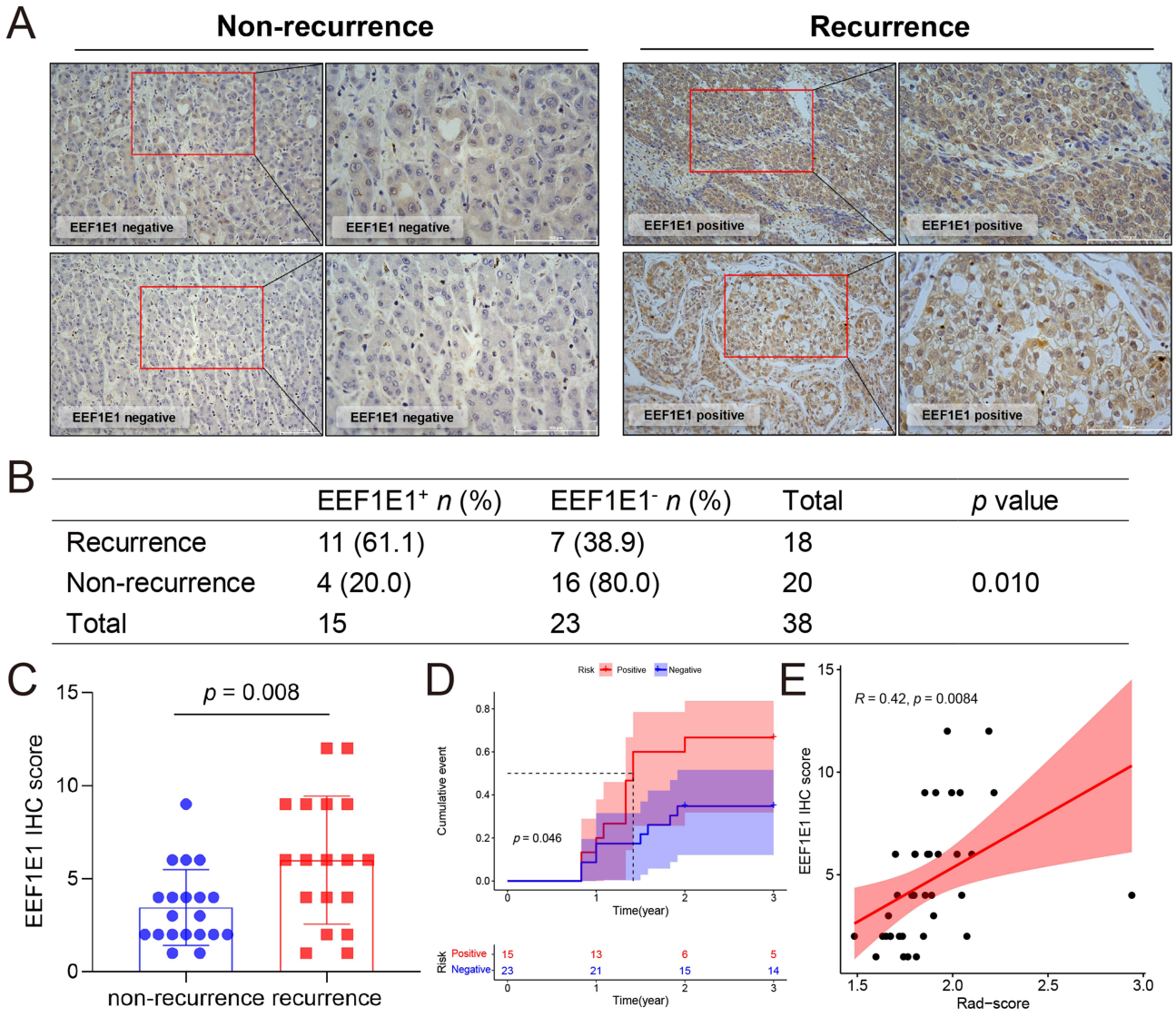

B	EEF1E1^{+} *n* (%)	EEF1E1^{-} *n* (%)	Total	*p* value
Recurrence	11 (61.1)	7 (38.9)	18	
Non-recurrence	4 (20.0)	16 (80.0)	20	0.010
Total	15	23	38	

Figure 5 Relation between EEF1E1 protein levels and HCC recurrence status. (**A**) IHC stains image of EEF1E1 protein levels in different recurrence risk of HCC tissues. (**B**) Statistical analysis was performed using the Chi-square test to compare the relative levels of EEF1E1 negative (EEF1E1^{-}) or positive (EEF1E1^{+}) between HCC with recurrence and HCC without recurrence (p = 0.010). (**C**) Boxplot of IHC scores of EEF1E1 between non-recurrence and recurrence patients. (**D**) Risk accumulation curve of EEF1E1 protein level for early recurrence in IHC validation cohort. (**E**) Correlation between Rad-scores and EEF1E1 IHC scores.

Discussion

In this study, we constructed and validated the Rad-score to assess the risk of early recurrence in patients with HCC. The results showed that it had a good predictive value for recurrence. Biological annotations suggested that radiomics features may be related to functions such as metabolism and immunity, and the brown module was highly positively correlated with the Rad-score (r = 0.64, $p < 0.001$). Therefore, we analyzed the genes in the brown module. We obtained five key radiomics genes (LRP12, GPD1L, GARS, EEF1E1, and DGKG) through the intersection of two independent datasets, based on which the fitted prognostic models were effective in predicting recurrence. Moreover, we introduced an IHC validation cohort to verify the correlation between EEF1E1 and Rad-score. These results suggest that the radiomics gene EEF1E1, which is derived from contrast-enhanced CT images of HCC patients, could serve as a biomarker for HCC recurrence prediction, and annotated pathways suggested that alterations in metabolic and immune microenvironments might be involved in HCC recurrence.

Previous studies have illustrated the molecular subtypes underlying different radiomics phenotypes in non-small cell lung cancer and glioblastoma.[23,24] Currently, research on HCC radiogenomics mainly focuses on the PI3K-mTOR

pathway or drug resistance mechanisms.[18,25] The CSVA analysis used in this study was based on whole transcriptome data, which could reflect pathway changes more comprehensively.[21] To assess the relationship between recurrence-related radiomics features or genes and immune cell infiltration, we used CIBRSORTS.[26] Furthermore, whether the infiltration of immune cells can be reflected through radiomics features in the future, the characteristics of the microenvironment of patients with HCC can be noninvasively evaluated in advance, which will provide sufficient evidence for the selection of immunotherapeutic targets for patients with HCC. Furthermore, we enrolled a cohort to validate the radiomics gene by performing IHC staining, and the results suggested a close relationship between Rad-scores and the radiomics gene, which represents genes derived from CT images that have a good stratification effect on prognosis.

For all extracted features, we first used the maximum correlation minimum redundancy (mRMR) method to screen the features of the stable part delineated by different radiologists, which was also used in a previous study.[27] We then used LASSO Cox to fit stable features to a Rad-score, which represents the patient's risk of early recurrence. Rad-score is constructed by six features, three of which are from the arterial phase and three from the portal phase, which are in line with the enhanced CT imaging features of HCC. In addition, each of these features has a certain predictive effect for the early recurrence of HCC; the C-index of wavelet LLH_gldm_DependenceNonUniformityNormalized (*V250*) was 0.731 (95% CI: 0.628–0.819), while the C-index of the Rad-score synthesized by these six features was 0.796 (95% CI: 0.702–0.884), which had advantages in comparison with the clinical parameters.

Notably, the biological pathways reflected by these six features focus on metabolism, proliferation, and immunity, which are closely related to the occurrence and development of HCC. At present, HCC patients benefit more from atezolizumab combined with bevacizumab than sorafenib,[28] which emphasizes the important role of the metabolic microenvironment represented by anti-angiogenesis and the immune microenvironment represented by anti-PD-L1 in HCC. A recent study showed that endothelial DGKG promotes tumor angiogenesis and immune evasion in HCC.[22] Since DGKG was also screened in this study, which justified the process we determined radiomics genes, it is also suggested that the recurrence of HCC is closely related to angiogenesis.

Although we demonstrated a correlation between CT images, gene expression, and HCC prognosis, further mechanisms remain to be validated. Using the brown module analyzed by WGCNA, we identified radiomics genes and analyzed the relationship between radiomics genes and immune microenvironments. LRP12 is also called LDL receptor-related protein 12, which is involved in the regulation of lipoxygenases in LDL oxidation;[29] GPD1L could catalyze the conversion of sn-glycerol 3-phosphate to glycerone phosphate, and has been reported as a potential predictive biomarker for HCC treatment outcomes.[30] Intriguingly, DGKG suppresses glucose transport and glycolysis by downregulating GLUT1 levels and plays a tumor suppressor role in HCC by inhibiting cell proliferation and migration.[31] Moreover, as mentioned above, hypoxia-induced EC-specific DGKG hyperexpression promotes tumor angiogenesis and immune evasion via the ZEB2/TGF-β1 axis in HCC.[22] EEF1E1, which is validated in this study, has been reported that the high EEF1E1 expression was found to be correlated with worse prognosis and may be associated with immune cell infiltration in HCC, and EEF1E1 may be participating in EEF1E1/ATM/p53 signaling pathway in HCC.[32] However, these findings require further verification. Moreover, the mechanism by which EEF1E1 influences recurrence remains unclear, although there are some limitations in this study.

Although our training cohort was composed predominantly of patients with HBV-related HCC, validation against the racially and etiologically heterogeneous TCGA cohort demonstrated that the imaging-genomic signature also captured fundamental biological processes such as lipid metabolism, hypoxia/angiogenesis, and immune modulation. This suggests that the model reflects common downstream hallmarks of HCC across HBV-, HCV-, and NAFLD-related disease. Nevertheless, we acknowledge that racial and etiologic differences may affect effect sizes, and therefore the TCGA validation should be interpreted as a conservative evaluation of transportability rather than definitive proof of generalizability. Multi-center studies within homogeneous HBV or NAFLD cohorts remain a necessary next step.

There were several limitations involved in this paper. First, the results of the radiomics model require multicenter validation with a large sample size. Second, the scarcity of samples and the differences in multicenter imaging protocols might have led to data heterogeneity, although we tried to avoid this problem as much as possible. In addition, detailed records of prior treatments were not available in TCGA, and although we excluded scans with iodized oil deposition to

minimize bias, residual confounding cannot be fully ruled out. Finally, the results of radiogenomics require additional approaches for validation, such as RNA-seq, single-cell RNA-seq, and Spatial transcriptomics.

Conclusions

In conclusion, we analyzed the imaging and transcriptomic data of HCC, explored its biological significance, and validated a radiomics gene at the protein level. Radiomics features not only have a good predictive effect on early recurrence but also may be related to several metabolic and immune-related processes in HCC recurrence.

Data Sharing Statements

The research data were stored in an institutional repository and shared upon request to the corresponding author.

Ethics Approval and Informed Consent

The studies involving human participants were reviewed and approved by the research ethics committee of the First Affiliated Hospital of Guilin Medical University and complied with The Declaration of Helsinki Principles. Written informed consent was obtained from all patients for their data to be used in the study.

Funding

This work was supported in part by the National Natural Science Foundation of China (No. 81773148 and 81772923), the National Key Sci-Tech Special Project of China (No. 2018ZX10302207), the Beijing Nova Program (No.20250484965), the Natural Science Foundation of Guangxi (No. 2018GXNSFDA138001), the Peking University Medicine Seed Fund for Interdisciplinary Research (No. BMU2021MX007, BMU2022MX001), and Fundamental Research Funds for the Central Universities, Peking University People's Hospital Scientific Research Development Funds (No. RDX2020-06, No. RDJ2022-14), the Program of the Guangxi Zhuang Autonomous Region Health and Family Planning Commission (No. Z20210706), Beijing Natural Science Foundation (No. 7222191), and the Qi-Min Project (grant number: NA.).

Disclosure

The authors declare no conflicts of interest in this work.

References

1. Sung H, Ferlay J, Siegel RL, et al. Global cancer statistics 2020: GLOBOCAN estimates of incidence and mortality worldwide for 36 cancers in 185 countries. *Ca a Cancer J Clinicians*. 2021;71(3):209–249. doi:10.3322/caac.21660
2. Tabrizian P, Jibara G, Shrager B, Schwartz M, Roayaie S. Recurrence of hepatocellular cancer after resection: patterns, treatments, and prognosis. *Ann Surg*. 2015;261(5):947–955. doi:10.1097/SLA.0000000000000710
3. Farinati F, Marino D, De Giorgio M, et al. Diagnostic and prognostic role of alpha-fetoprotein in hepatocellular carcinoma: both or neither? *Am J Gastroenterol*. 2006;101(3):524–532. doi:10.1111/j.1572-0241.2006.00443.x
4. Yang SL, Liu LP, Yang S, et al. Preoperative serum α-fetoprotein and prognosis after hepatectomy for hepatocellular carcinoma. *Br J Surg*. 2016;103(6):716–724. doi:10.1002/bjs.10093
5. Giannini EG, Marenco S, Borgonovo G, et al. Alpha-fetoprotein has no prognostic role in small hepatocellular carcinoma identified during surveillance in compensated cirrhosis. *Hepatology*. 2012;56(4):1371–1379. doi:10.1002/hep.25814
6. Ji G-W, Zhu F-P, Xu Q, et al. Radiomic features at contrast-enhanced CT predict recurrence in early stage hepatocellular carcinoma: a multi-institutional study. *Radiology*. 2020;294(3):568–579. doi:10.1148/radiol.2020191470
7. Akai H, Yasaka K, Kunimatsu A, et al. Predicting prognosis of resected hepatocellular carcinoma by radiomics analysis with random survival forest. *Diagn Interventional Imaging*. 2018;99(10):643–651. doi:10.1016/j.diii.2018.05.008
8. Wakabayashi T, Ouhmich F, Gonzalez-Cabrera C, et al. Radiomics in hepatocellular carcinoma: a quantitative review. *Hepatol Internat*. 2019;13(5):546–559. doi:10.1007/s12072-019-09973-0
9. Lambin P, Rios-Velazquez E, Leijenaar R, et al. Radiomics: extracting more information from medical images using advanced feature analysis. *Eur J Cancer*. 2012;48(4):441–446. doi:10.1016/j.ejca.2011.11.036
10. Lambin P, Leijenaar RTH, Deist TM, et al. Radiomics: the bridge between medical imaging and personalized medicine. *Nat Rev Clin Oncol*. 2017;14(12):749–762. doi:10.1038/nrclinonc.2017.141
11. Lee S, Kang TW, Song KD, et al. Effect of microvascular invasion risk on early recurrence of hepatocellular carcinoma after surgery and radiofrequency ablation. *Ann Surg*. 2021;273(3):564–571. doi:10.1097/SLA.0000000000003268
12. Li Y, Zhang Y, Fang Q, et al. Radiomics analysis of [18F]FDG PET/CT for microvascular invasion and prognosis prediction in very-early- and early-stage hepatocellular carcinoma. *Eur J Nucl Med Mol Imaging*. 2021;48(8):2599–2614. doi:10.1007/s00259-020-05119-9

13. Ma X, Wei J, Gu D, et al. Preoperative radiomics nomogram for microvascular invasion prediction in hepatocellular carcinoma using contrast-enhanced CT. *Eur Radiol*. 2019;29(7):3595–3605. doi:10.1007/s00330-018-5985-y
14. Xu X, Zhang H-L, Liu Q-P, et al. Radiomic analysis of contrast-enhanced CT predicts microvascular invasion and outcome in hepatocellular carcinoma. *J Hepatol*. 2019;70(6):1133–1144. doi:10.1016/j.jhep.2019.02.023
15. Hu H-T, Wang Z, Huang X-W, et al. Ultrasound-based radiomics score: a potential biomarker for the prediction of microvascular invasion in hepatocellular carcinoma. *Eur Radiol*. 2019;29(6):2890–2901. doi:10.1007/s00330-018-5797-0
16. Feng S-T, Jia Y, Liao B, et al. Preoperative prediction of microvascular invasion in hepatocellular cancer: a radiomics model using Gd-EOB-DTPA-enhanced MRI. *Eur Radiol*. 2019;29(9):4648–4659. doi:10.1007/s00330-018-5935-8
17. Zhang Z, Jiang H, Chen J, et al. Hepatocellular carcinoma: radiomics nomogram on gadoxetic acid-enhanced MR imaging for early postoperative recurrence prediction. *Cancer Imaging*. 2019;19(1):22. doi:10.1186/s40644-019-0209-5
18. Liao H, Jiang H, Chen Y, et al. Predicting genomic alterations of phosphatidylinositol-3 kinase signaling in hepatocellular carcinoma: a radiogenomics study based on next-generation sequencing and contrast-enhanced CT. *Ann Surg Oncol*. 2022. doi:10.1245/s10434-022-11505-4
19. Clark K, Vendt B, Smith K, et al. The Cancer Imaging Archive (TCIA): maintaining and operating a public information repository. *J Digital Imaging*. 2013;26(6):1045–1057. doi:10.1007/s10278-013-9622-7
20. Ren L, Chen D, Xu W, et al. Predictive potential of Nomogram based on GMWG for patients with hepatocellular carcinoma after radical resection. *BMC Cancer*. 2021;21(1):817. doi:10.1186/s12885-021-08565-2
21. Hänzelmann S, Castelo R, Guinney J. GSVA: gene set variation analysis for microarray and RNA-seq data. *BMC Bioinf*. 2013;14(7). doi:10.1186/1471-2105-14-7
22. Zhang L, Xu J, Zhou S, et al. Endothelial DGKG promotes tumor angiogenesis and immune evasion in hepatocellular carcinoma. *J Hepatol*. 2024;80(1):82–98. doi:10.1016/j.jhep.2023.10.006
23. Zhou M, Leung A, Echegaray S, et al. Non-small cell lung cancer radiogenomics map identifies relationships between molecular and imaging phenotypes with prognostic implications. *Radiology*. 2018;286(1):307–315. doi:10.1148/radiol.2017161845
24. Sun Q, Chen Y, Liang C, et al. Biologic pathways underlying prognostic radiomics phenotypes from paired MRI and RNA sequencing in glioblastoma. *Radiology*. 2021;301(3):654–663. doi:10.1148/radiol.2021203281
25. Kuo MD, Gollub J, Sirlin CB, Ooi C, Chen X. Radiogenomic analysis to identify imaging phenotypes associated with drug response gene expression programs in hepatocellular carcinoma. *J Vasc Intervent Radiol*. 2007;18(7):821–831. doi:10.1016/j.jvir.2007.04.031
26. Newman AM, Liu CL, Green MR, et al. Robust enumeration of cell subsets from tissue expression profiles. *Nat Meth*. 2015;12(5):453–457. doi:10.1038/nmeth.3337
27. L E, Li L, Lu L, et al. Radiomics for classification of lung cancer histological subtypes based on nonenhanced computed tomography. *Acad Radiol*. 2019;26(9):1245–1252. doi:10.1016/j.acra.2018.10.013
28. Finn RS, Qin S, Ikeda M, et al. Atezolizumab plus bevacizumab in unresectable hepatocellular carcinoma. *New Engl J Med*. 2020;382(20):1894–1905. doi:10.1056/NEJMoa1915745
29. Takahashi Y, Zhu H, Yoshimoto T. Essential roles of lipoxygenases in LDL oxidation and development of atherosclerosis. *Antioxid Redox Signaling*. 2005;7(3–4):425–431. doi:10.1089/ars.2005.7.425
30. Leung PKH, Das B, Cheng X, Tarazi M. Prognostic and predictive utility of GPD1L in human hepatocellular carcinoma. *Int J Mol Sci*. 2023;24(17). doi:10.3390/ijms241713113
31. Guo Z, Jia J, Yao M, et al. Diacylglycerol kinase γ predicts prognosis and functions as a tumor suppressor by negatively regulating glucose transporter 1 in hepatocellular carcinoma. *Exp Cell Res*. 2018;373(1–2):211–220. doi:10.1016/j.yexcr.2018.11.001
32. Han R, Feng P, Pang J, et al. A novel HCC prognosis predictor EEF1E1 is related to immune infiltration and may be involved in EEF1E1/ATM/p53 signaling. *Front Oncol*. 2021;11. doi:10.3389/fonc.2021.700972

Journal of Hepatocellular Carcinoma

Dovepress
Taylor & Francis Group

Publish your work in this journal

The Journal of Hepatocellular Carcinoma is an international, peer-reviewed, open access journal that offers a platform for the dissemination and study of clinical, translational and basic research findings in this rapidly developing field. Development in areas including, but not limited to, epidemiology, vaccination, hepatitis therapy, pathology and molecular tumor classification and prognostication are all considered for publication. The manuscript management system is completely online and includes a very quick and fair peer-review system, which is all easy to use. Visit http://www.dovepress.com/testimonials.php to read real quotes from published authors.

Submit your manuscript here: https://www.dovepress.com/journal-of-hepatocellular-carcinoma-journal